A&A 390, 1153–1170 (2002)
DOI: 10.1051/0004-6361:20020478

Astronomy & Astrophysics

Spectroscopy of large PAHs

Laboratory studies and comparison to the Diffuse Interstellar Bands

R. Ruiterkamp[1], T. Halasinski[2], F. Salama[2], B. H. Foing[3], L. J. Allamandola[2], W. Schmidt[4], and P. Ehrenfreund[1]

[1] Leiden Observatory, PO Box 9513, 2300 RA Leiden, The Netherlands
[2] Space Science Division, NASA-Ames Research Center, Moffett Field CA 94035, USA
[3] ESA Research Support Division, ESTEC/SCI-SR, PO Box 229, 2200 AG, Noordwijk, The Netherlands
[4] PAH Forschungs Institut, Flurstrasse 17, 86926 Greifenberg/Ammersee, Germany

Received 16 January 2002 / Accepted 27 March 2002

Abstract. Polycyclic Aromatic Hydrocarbons (PAHs) are thought to be the carriers of the ubiquitous infrared emission bands (UIBs). Data from the Infrared Space Observatory (ISO) have provided new insights into the size distribution and the structure of interstellar PAH molecules pointing to a trend towards larger-size PAHs. The mid-infrared spectra of galactic and extragalactic sources have also indicated the presence of 5-ring structures and PAH structures with attached side groups. This paper reports for the first time the laboratory measurement of the UV–Vis–NIR absorption spectra of a representative set of large PAHs that have also been selected for a long duration exposure experiment on the International Space Station ISS. PAHs with sizes up to 600 amu, including 5-ring species and PAHs containing heteroatoms, have been synthesized and their spectra measured using matrix isolation spectroscopy. The spectra of the neutral species and the associated cations and anions measured in this work are also compared to astronomical spectra of Diffuse Interstellar Bands (DIBs).

Key words. molecular data – methods: laboratory – ISM: lines and bands – ISM: molecules

1. Introduction

A substantial fraction of the ca. 120 gas phase molecules that have been identified in interstellar and circumstellar regions are organic in nature (Ehrenfreund & Charnley 2000). Most of these molecules have been detected through their rotational lines. Large carbon-bearing molecules (such as polycyclic aromatic hydrocarbons (PAHs), fullerenes and unsaturated chains) are also thought to be present in the interstellar medium (ISM). These large molecules are difficult to identify in the radio range and can only be detected through their electronic or vibrational signature in the UV-Vis-IR range.

The presence of large aromatic structures is evidenced by infrared observations of the ISM in our galaxy and in extragalactic environments (see A&A Vol. 315, 1996) and by the observation of the Diffuse Interstellar Bands (DIBs) in the visible range (see Herbig 1995 for a review, Tielens & Snow 1995). Hydrogenated amorphous carbon (HAC) is considered a potential carrier for the 2200 Å bump observed in the interstellar extinction curve (Mennella et al. 1999), while a variety of complex aromatic networks are likely to be present on carbonaceous grains (see Henning & Salama 1998 for a review). Since the initial discovery of simple diatomic molecules in interstellar space (Swings & Rosenfeld 1937; McKellar 1940; Douglas & Herzberg 1941); many more molecules have been detected in the diffuse medium, such as HCO^+, CO, OH, C_2, HCN, CN, CS and H_2CO (Lucas & Liszt 1997). Models of gas-phase reactions in diffuse clouds predict that organic molecules can be formed through ion-molecule reactions and neutral-neutral reactions in the diffuse medium (Bettens & Herbst 1996). Aromatic and unsaturated linear carbon molecules of up to 64 C atoms have been predicted by these models (Herbst 1995; Ruffle et al. 1999). Reactions in circumstellar envelopes and subsequent mixing into the diffuse medium, photochemical reactions and grain collisions in carbonaceous dust are alternative processes that can also lead to the formation of organic molecules.

Here, we report the spectroscopy of large PAHs (see Fig. 1). Although extensive laboratory studies have been performed on the spectroscopy of smaller PAHs (i.e., <25 C-atoms molecules) in an astrophysical context, almost no information is available regarding large PAHs (>25 C atoms, for a recent review see Salama 1999).

The PAH molecules shown in Fig. 1 have also been selected for a long duration exposure experiment "Organic Matter in Space" on the International Space Station (ISS) (Ruiterkamp et al. 2001). This space experiment will provide quantitative data on the photochemical evolution of specific PAH species in irradiated environments. The results will help to constrain the formation and destruction pathways of large carbonaceous

Send offprint requests to: R. Ruiterkamp,
e-mail: ruiterka@strw.leidenuniv.nl

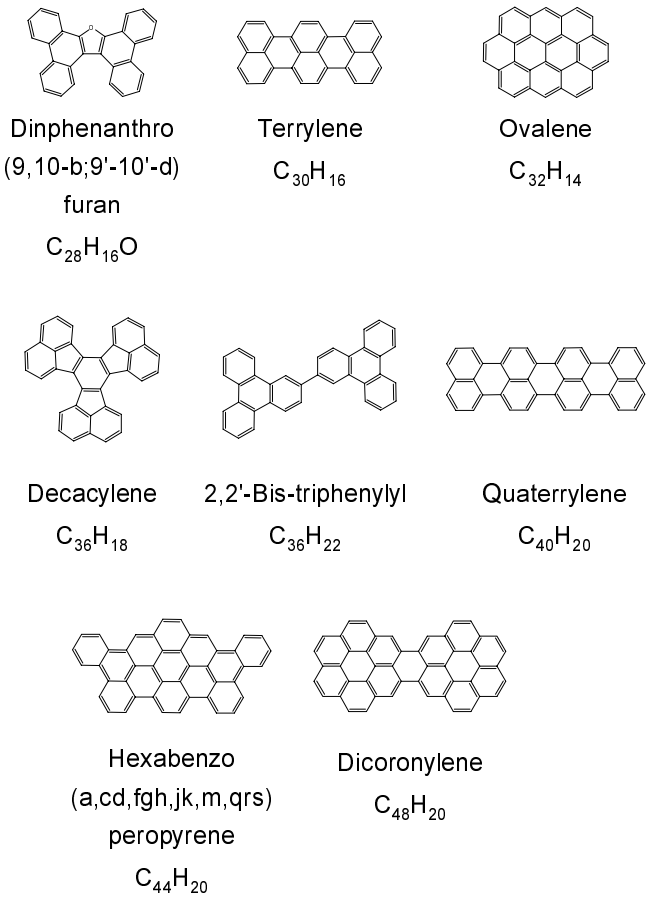

Fig. 1. Structural formulae of the Polycyclic Aromatic Hydrocarbon molecules studied by UV-Vis-NIR spectroscopy.

molecules in interstellar and interplanetary media. The sample set includes regular compact and non-compact PAHs (i.e., structures made only of benzenoid rings), PAH structures with 5-membered rings as well as one oxygen-bearing PAH.

Thus, the objectives of this work are: (i) to explore for the first time the electronic spectroscopy of large PAH molecules and ions in an environment that is astrophysically relevant for comparison with the spectra of DIBs; (ii) to identify promising target molecules for further studies in gas-phase, jet expansion, experiments; (iii) to study the photo-stability of these selected species in the laboratory for a comparison with samples to be exposed on the ISS.

In Sect. 2 we briefly review the evidence pointing toward the presence of PAHs in the ISM and the potential connection to the DIBs. In Sect. 3 we describe the laboratory setup used in this study. In Sect. 4 we report and discuss the UV-Vis-NIR absorption spectra of selected large, neutral and ionized, PAH molecules in the astrophysical context. The spectra are finally compared with high resolution DIB data in Sect. 5.

2. The carrier molecules of the diffuse interstellar bands

2.1. The Diffuse Interstellar Bands

Diffuse Interstellar Bands (DIBs) are absorption lines that are detected in the spectra of reddened stars throughout our galaxy. They are observed in a spectral range extending from the UV to the near-IR, and they exhibit a large diversity of band strengths and profiles (Herbig 1995). The detection of DIBs in almost all regions of the diffuse ISM indicates that the carriers are chemically stable.

High resolution surveys of the DIBs indicate that the band strengths depend on the environmental conditions that prevail in the ISM (Herbig 1975; Cami et al. 1997; Sonnentrucker et al. 1997). The DIB carriers are strongly influenced by the UV field. The shielding of UV radiation by the outer layers of the clouds leads to a progressive reduction of DIB strength towards the interior of the cloud (Cami et al. 1997).

The current consensus based on both astronomical observations and laboratory studies is that the DIB carriers are gas phase molecules that are chemically stable and carbonaceous in nature (Herbig 1995; Tielens & Snow 1995; Henning & Salama 1998; Ehrenfreund & Charnley 2000; Ehrenfreund et al. 2001). The observation of some DIBs in emission in the Red Rectangle (Sarre et al. 1995) and the detection of intrinsic substructures in several of the stronger DIBs marked a breakthrough in the identification of the molecular nature of the DIB carriers (Sarre et al. 1995; Ehrenfreund & Foing 1996; Krelowski et al. 1998; Le Coupanec et al. 1999; Walker et al. 2001).

2.2. Proposed carbonaceous carriers

Among the potential DIB carriers are stable carbonaceous molecules such as PAHs, fullerenes, carbon chains and rings. In order to identify the carrier molecules of DIBs, laboratory studies have been carried out on PAHs (Salama et al. 1996; Salama et al. 1999) and carbon chains (Freivogel et al. 1994; Tulej et al. 1998). There is, however, no definitive identification of one specific carrier for any of the 300 known DIBs. It seems logical to seek the carriers of the DIBs among interstellar molecules that are both stable and cosmically abundant. In this report we focus on PAHs. The spectroscopy of large fullerenes will be discussed in a separate paper. PAHs are believed to be the most abundant free organic molecules in space (Puget & Leger 1989; Allamandola et al. 1989) and to be formed in the outer atmosphere of carbon stars, or by shock fragmentation of carbonaceous solid material. The infrared emission bands (UIBs) measured at 3.3, 6.2, 7.7, 8.6, 11.2 and 12.7 μm are ubiquitous in space. The bands are observed in the diffuse interstellar medium, in circumstellar environments and even in external galaxies (Tielens et al. 1999). UIBs have been successfully modeled by combining the infrared laboratory absorption spectra of neutral and positively charged PAHs (Hudgins & Allamandola 1999a, b).

PAHs play an important role in the evolution of interstellar gas phase chemistry (Bakes & Tielens 1994). Gaseous PAH molecules react according to the environmental conditions. Neutral and hydrogenated PAHs are present in dense regions and regions of high electron density. The local ultraviolet radiation field determines their charge and their hydrogenation states (Salama et al. 1996; Sonnentrucker et al. 1997; Vuong & Foing 2000). Furthermore, the UV-Vis spectra of PAH cations

with up to 100 C atoms show strong absorption bands. This makes PAHs promising candidates for the molecular carriers of the diffuse interstellar bands. The search for specific bands of PAH cations in highly reddened stars has shown some similarities with the spectra of small PAHs measured in the laboratory in neon matrices but no definitive identification can be made until astrophysically relevant gas-phase data are available. Although PAHs appear to be potential carrier molecules, other species have to be explored, e.g. fullerenes such as the cation C_{60}^{+} have been discussed (Foing & Ehrenfreund 1994; Foing & Ehrenfreund 1997). Laboratory spectroscopy experiments provide a vital tool for the identification of the DIB carriers in the ISM.

3. Experimental

The molecules used in this study were synthesized via condensation processes of small units (e.g. naphthalene) according to well established literature methods (Clar 1964). The laboratory spectra were obtained at NASA-Ames using the techniques of Matrix Isolation Spectroscopy (MIS). This technique approximates the known (or expected) environmental conditions of the diffuse interstellar medium in the laboratory. In MIS experiments, neutral and ionized PAHs are fully isolated in low-polarizability neon matrices at <5 K. The induced perturbations – in terms of peak position and profile of the bands – in the spectra of the neutral/ionized PAHs are minimal (Salama 1996). The experimental apparatus and protocol have been described previously (Salama et al. 1999), and here we only provide a brief description. A sample holder is suspended in the center of a sample chamber that is part of a high vacuum system. The sample chamber consists of four ports at 90° and a gas injection port at 45°. The sample holder is cooled to 4.2 K using a liquid Helium transfer cryostat. The substrate can be rotated to face a vacuum deposition furnace, the spectroscopy ports, a VUV irradiation lamp and the inert gas injection port, respectively. Spectra of the isolated PAH molecules were obtained with a 0.5-m, triple grating monochromator and a CCD array mounted on the exit port, and interfaced to a computer system. The spectral light sources consist of a D_2 lamp (UV) and a tungsten filament lamp (Vis - NIR). The light collected at the spectroscopy port of the sample chamber is directed to the entrance slit of the monochromator by a fiber optic cable. The wavelength coverage of the spectrometer system is 180–1200 nm. Wavelength calibration of the spectrometer is provided by the emission lines of a neon and a Mercury lamp. The mean of the deviation compared to literature values was used to calibrate the entire spectrum. Calibration shifts did not exceed 0.05 nm.

A microwave-powered, flow-discharge hydrogen lamp generating 10.2 eV photons (L_α) is used for irradiation. Note that in the case of large molecules with low ionization potential (IP), the Deuterium lamp also can ionize the sample before irradiation with L_α. In typical experiments, PAH samples are simultaneously condensed with the neon gas onto the cold substrate, and the frozen matrix is then spectroscopically probed. The matrix is then exposed to VUV irradiation leading to the formation of ions from the neutral precursor and the observation of new spectral features in the UV-NIR range (180–1200 nm). The new features are associated with the formation of ions in the matrix through one-photon ionization of the neutral PAH precursor. All samples were irradiated for 10 min leading to the formation of cation and anion pairs in the neon matrix. Additional experiments were performed in each case to discriminate between the spectral signatures of the ion and its counter ion. This was done by doping the matrix with an electron scavenger, NO_2, to ensure that only cations were formed in the matrix (Jacox 1978). Comparison between the two sets of experiments allows an unambiguous determination of the signature associated with each ion and its counter ion in the matrix. The spectra of matrices doped with NO_2 exhibit NO_2 bands that peak at 570 nm, 604 nm and 643 nm. These features have been omitted from the tables in the results section. Although all features above the 0.02 absorption level have been taken into account, a few broad features falling above 1100 nm with residuals at the 0.02 absorbance level (probably due to matrix effects) have been omitted from the discussion.

4. Results and discussion

Figures 2 to 9 show the absorption spectra of neutral and ionized PAHs. Note that for each figure, the left panel shows the absorption spectrum of the matrix-isolated neutral PAH while the right panel shows the spectrum derived from the difference between the spectra of the same PAH measured before and after irradiation of the matrix respectively.

The "difference spectrum" is defined as the negative logarithm of the single beam intensity associated with the ionized species divided by the single beam intensity associated with the neutral species. The difference spectra show a negative absorbance for the neutral precursor that is depleted into ions and a positive absorbance for the ions that are produced. The tables list the peak positions, Full Width at Half Maximum (*FWHM*) and peak heights of the bands measured in the laboratory.

4.1. Neutral and ionized diphenanthrofuran $C_{28}H_{16}O$

The absorption spectrum of neutral diphenanthrofuran is shown in Fig. 2. The spectrum is characterized by a broad absorption band system peaking at 262.5 nm and two band systems with pronounced fine structure seen around 331.0 nm and 360 nm, respectively. Upon photolysis, seven new additional features appear in the spectrum. The new features include a band system comprised of three peaks centered near 426.0 nm and a multiple peak structure centered around 618.4 nm. Comparison of this spectrum with the results of a Ne/NO_2 experiment shows that a peak seen at 752.8 after VUV irradiation is absent when the Ne matrix is doped with NO_2. The 752.8 nm band can therefore be confidently assigned to the anion of diphenanthrofuran $C_{28}H_{16}O^{-}$. The peak position, intensity and *FWHM* for each band are given in Table 1.

4.2. Neutral and ionized terrylene $C_{30}H_{16}$

The spectrum of neutral terrylene (Fig. 3) shows a broad band system around 220 nm and a narrower, strong, absorption band system with substructure in the visible (450–600 nm

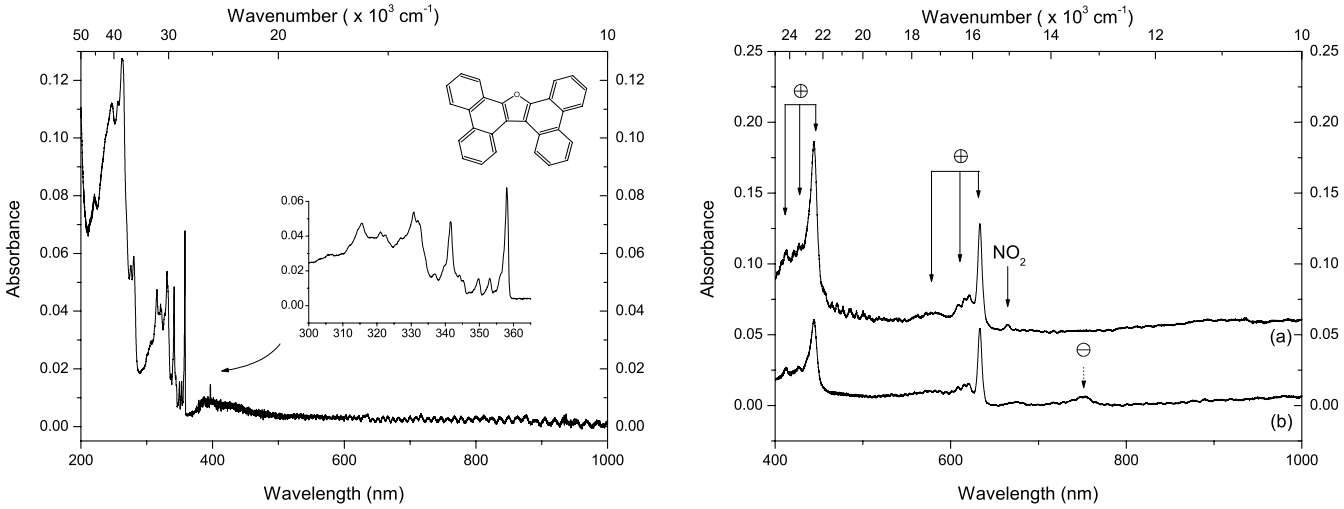

Fig. 2. Comparison of the spectral features associated with neutral (left panel) and VUV-irradiated (right panel) diphenanthrofuran (Dp) isolated in neon (Ne) and in Ne/NO_2 matrices. **a)** is the spectrum of the photolysis products in a neon/NO_2 matrix; **b)** is the spectrum of the photolysis products, including Dp^+ and Dp^-, in a neon matrix. Band peak positions, intensities and *FWHM* are reported in Table 1.

Table 1. Absorption features associated with the UV/Vis/NIR spectra of neutral and ionized diphenanthrofuran ($C_{28}H_{16}O$) isolated at 4 K in inert-gas matrices.

Neutral in neon matrix			10 min. irr. in neon matrix			10 min. irr. in neon/NO_2 matrix		
Peak pos. (nm)	*FWHM* (nm)	Abs_{max}	Peak pos. (nm)	*FWHM* (nm)	Abs_{max}	*FWHM* (nm)	Abs_{max}	Assignment
220.95 (B)	6.6	0.099	413.37	4.9	0.009	6.8	0.007	+
246.67 (B)	6.2	0.112	425.99	4.3	0.027	2.9	0.064	+
256.46 (B)	3.9	0.113	444.43	10.3	0.055	7.4	0.134	+
262.51 (B)	7.9	0.130	578.26	43.7	0.004	37.3	0.006	+
275.79 (B)	2.4	0.056	617.36	11.4	0.015	6.1	0.026	+
280.25 (B)	4.5	0.059	633.17	4.9	0.053	5.5	0.075	+
315.40 (B)	1.7	0.047	752.82	19.5	0.006			-
321.01 (B)	1.0	0.042						
331.04 (B)	5.3	0.052						
336.75 (B)	2.1	0.018						
341.46 (B)	1.1	0.048						
349.57	1.0	0.015						
352.94	0.9	0.015						
357.92	0.9	0.066						
1073.70	3.6	0.010						

(B) = Blended peak. Assignments only apply to the peaks that are detected in the spectra of the irradiated sample. + = cation; - = anion.

range). VUV irradiated terrylene exhibits new absorptions including two strong bands at 690.4 nm and 741.3 nm. A close comparison of the spectra with the spectrum of a Ne/NO_2-doped matrix shows that the 741.3 nm band belongs to the anion as well as a few other, weaker, features. The values for the peak positions, intensities and *FWHM* are given in Table 2.

4.3. Neutral and ionized ovalene $C_{32}H_{14}$

Three major absorption band systems are seen in the spectrum of neutral ovalene shown in Fig. 4. A broad absorption peaking around 215.8 nm, a band system falling in the 270–340 nm range and another, narrower, band system falling between 340 and 430 nm. This spectrum is in agreement with the information available in the literature (Ehrenfreund et al. 1992). After exposure to VUV irradiation, the main new features that arise in the spectrum peak at 463.2, 535.7, 562.1 and 974.9 nm. Band peak positions, intensities and *FWHM* are reported in Table 3.

4.4. Neutral and ionized decacyclene $C_{36}H_{18}$

The spectrum of neutral decacyclene isolated in a neon matrix is shown in Fig. 5. The spectrum is composed of two broad absorption band systems centered around 251.8 and 364.2 nm, respectively with superimposed fine structure. New broad bands

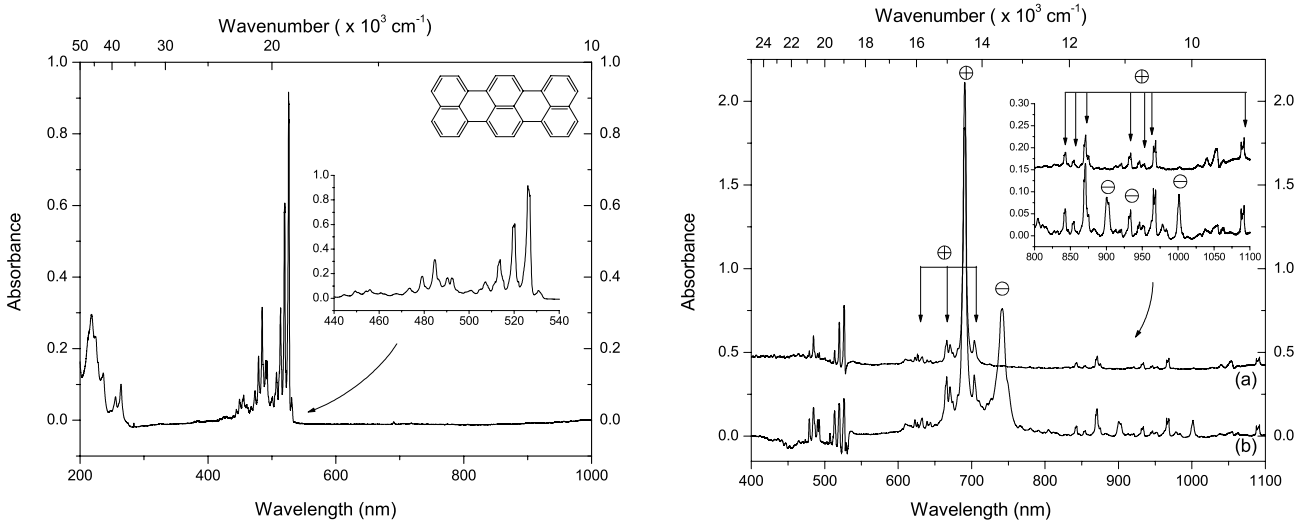

Fig. 3. Comparison of the spectral features associated with neutral (left panel) and VUV-irradiated (right panel) terrylene (Te) isolated in neon (Ne) and in Ne/NO_2 matrices. **a)** is the spectrum of the photolysis products in a neon/NO_2 matrix; **b)** is the spectrum of the photolysis products, including Te^+ and Te^-, in a neon matrix. Band peak positions, intensities and *FWHM* are reported in Table 2.

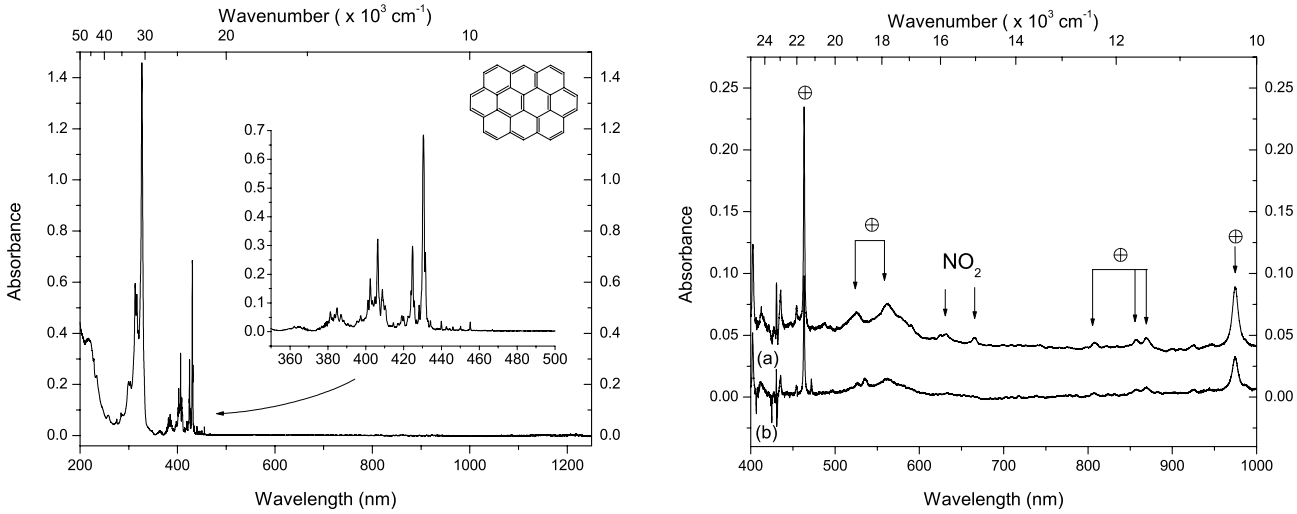

Fig. 4. Comparison of the spectral features associated with neutral (left panel) and VUV-irradiated (right panel) ovalene (Ov) isolated in neon (Ne) and in Ne/NO_2 matrices. **a)** is the spectrum of the photolysis products in a neon/NO_2 matrix; **b)** is the spectrum of the photolysis products in a neon matrix. Band peak positions, intensities and *FWHM* are reported in Table 3.

appear at 539.7, 813.0 and 1095.8 after VUV irradiation of decacyclene in a Ne/NO_2 matrix. All the bands are assigned to the decacyclene cation ($C_{36}H_{18}^+$). Band peak positions, intensities and *FWHM* are reported in Table 4.

4.5. Neutral and ionized 2, 2′-bis-triphenylyl $C_{36}H_{22}$

The spectrum of neutral triphenylyl (Fig. 6) shows strong absorption bands in the 200–350 nm range. In the case of the VUV-irradiated sample, both triphenylyl/Ne and triphenylyl/Ne/NO_2 experiments exhibit two strong bands near 457.7 and 490.4 nm, respectively, associated with the formation of the cation ($C_{36}H_{22}^+$) in the matrix. Band peak positions, intensities and *FWHM* are reported in Table 5.

4.6. Neutral and ionized quaterrylene $C_{40}H_{20}$

The spectrum of neutral quaterrylene (Fig. 7) exhibits a complex band system between 200 and 320 nm. A strong absorption band system is also found in the visible range between 450 and 660 nm with a peak at 607.9 nm. VUV irradiation of quaterrylene leads to the appearance of two new, strong, absorption bands located at 833.7 nm and 881.8 nm, respectively, together with weaker features down to the 1100 nm range. Comparison with the spectrum of a Ne/NO_2 matrix experiment indicates that the strong 881.8 nm band is associated with the absorption of the quaterrylene anion. Band peak positions, intensities and *FWHM* are reported in Table 6.

Note that the spectrum of neutral quaterrylene (Fig. 7) resembles closely that of neutral terrylene (Fig. 3), the only difference being the shift in band positions. The bands of

Table 2. Absorption features associated with the UV/Vis/NIR spectra of neutral and ionized terrylene ($C_{30}H_{16}$) isolated at 4 K in inert-gas matrices.

Neutral in neon matrix			10 min. irr. in neon matrix			10 min. irr. in neon/NO_2 matrix		
Peak pos. (nm)	*FWHM* (nm)	Abs_{max}	Peak pos. (nm)	*FWHM* (nm)	Abs_{max}	*FWHM* (nm)	Abs_{max}	Assignment
217.68 (B)	11.6	0.298	609.96	3.0	0.074	5.8	0.049	+
223.61 (B)	5.9	0.249	622.87	1.5	0.098	1.9	0.060	+
235.06 (B)	6.7	0.145	626.20	0.9	0.032	0.9	0.041	+
255.33 (B)	2.5	0.079	627.13	0.3	0.015	0.4	0.027	+
263.66 (B)	3.3	0.108	632.16	2.6	0.107	3.7	0.062	+
428.82	17.4	0.022	639.43	1.7	0.088	1.7	0.046	+
439.74	3.1	0.025	643.90	1.9	0.082	2.6	0.04	+
444.77	2.5	0.042	664.62	3.7	0.123	4.9	0.277	+
449.88	3.2	0.068	670.68	2.2	0.293	2.2	0.136	+
455.86	0.9	0.085	674.23	2.1	0.208	2.0	0.089	+
460.80	3.6	0.054	690.39	4.4	1.908	3.4	1.712	+
467.77	3.2	0.051	703.90	2.8	0.358	3.6	0.156	+
473.54	2.6	0.092	741.32	10.9	0.722			-
479.14	1.4	0.193	842.28	3.2	0.060	2.8	0.029	+
484.78	1.5	0.328	854.05	3.3	0.031	3.1	0.010	+
490.36	1.2	0.182	870.39	3.2	0.162	3.8	0.063	+
492.41	1.5	0.181	874.97	1.9	0.049	2.1	0.029	+
500.28	3.2	0.075	901.48	5.9	0.086			-
507.27	1.9	0.144	932.65	3.4	0.051	3.5	0.023	+
513.47	1.7	0.314	946.11	1.4	0.030	5.3	0.015	+
519.79	1.5	0.637	966.74	4.1	0.091	1.0	0.047	+
526.32	1.6	0.951	978.42	3.8	0.024			-
530.83	2.8	0.072	983.29	4.4	0.014			-
			1001.20	3.5	0.088			-
			1090.00	7.4	0.053	4.7	0.034	+

(B) = Blended peak. Assignments only apply to the peaks that are detected in the spectra of the irradiated sample. + = cation. - = anion.

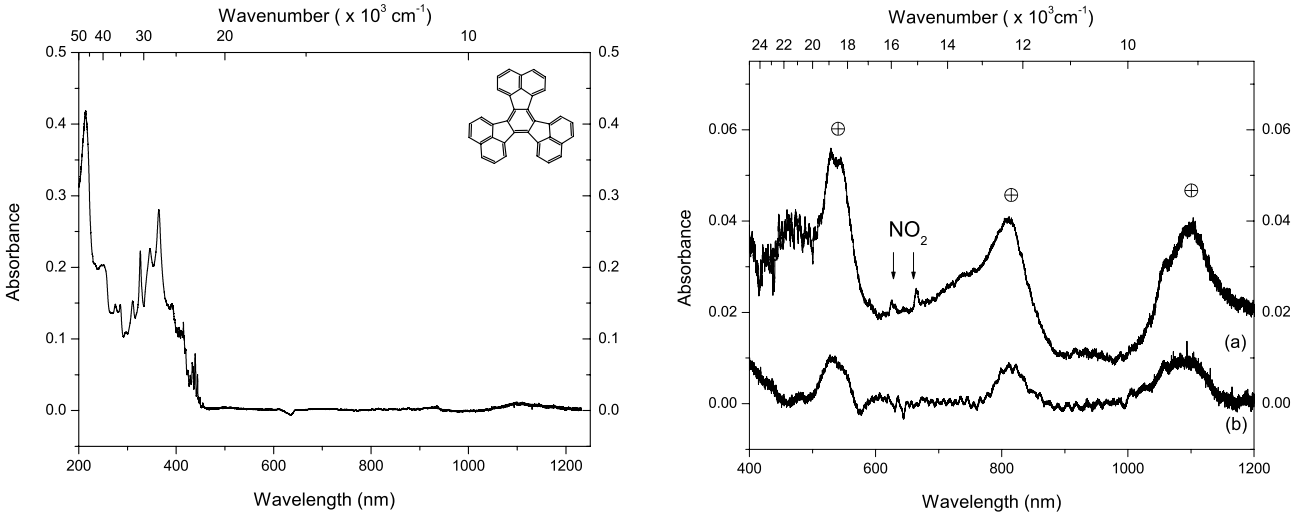

Fig. 5. Comparison of the spectral features associated with neutral (left panel) and VUV-irradiated (right panel) decacyclene (Dc) isolated in neon (Ne) and in Ne/NO_2 matrices. **a)** is the spectrum of the photolysis products in a neon/NO_2 matrix; **b)** is the spectrum of the photolysis products in a neon matrix. Band peak positions, intensities and *FWHM* are reported in Table 4.

quaterrylene are red-shifted compared to the bands of terrylene. The same effect is observed when comparing the spectra of their respective ions. This molecular size-related effect is well known and has been discussed in the literature (e.g. Clar 1964; Salama et al. 1996).

4.7. Neutral and ionized hexabenzoperopyrene $C_{44}H_{20}$

The spectrum of neutral hexabenzoperopyrene (Fig. 8) shows three band systems peaking at 236.0, 345.9, and 400.0 nm,

Table 3. Absorption features associated with the UV/Vis/NIR spectra of neutral and ionized ovalene ($C_{32}H_{14}$) isolated at 4 K in inert-gas matrices.

Neutral in neon matrix			10 min. irr. in neon matrix			10 min. irr. in neon/NO_2 matrix		
Peak pos. (nm)	*FWHM* (nm)	Abs_{max}	Peak pos. (nm)	*FWHM* (nm)	Abs_{max}	*FWHM* (nm)	Abs_{max}	Assignment
215.81 (B)	31.1	0.378	454.26	1.2	0.010	1.4	0.013	+
257.46 (B)	6.4	0.080	463.23	1.3	0.097	1.5	0.182	+
275.21	1.1	0.063	471.91	0.9	0.010			-
284.18	0.3	0.088	526.04	6.4	0.004	10.2	0.008	+
299.36 (B)	5.1	0.209	535.71	4.5	0.015			-
303.83 (B)	2.8	0.180	562.08	41.7	0.013	38.2	0.027	+
313.17 (B)	2.9	0.566	808.24	9.4	0.003	6.4	0.004	+
316.81 (B)	2.3	0.532	857.44	8.3	0.006	6.7	0.006	+
319.34 (B)	2.6	0.410	869.56	8.7	0.008	6.7	0.008	+
326.97	3.8	1.341	974.92	7.2	0.031	8	0.046	+
384.34	8.1	0.057	1074.75	11.7	0.011			-
395.60	1.4	0.036	1125.45	48.8	0.015	26.1	0.03	+
397.34	0.5	0.057						
402.41	0.4	0.184						
406.33	0.6	0.326						
408.85	1.2	0.137						
414.60	0.5	0.031						
417.05	0.9	0.028						
419.08	0.7	0.057						
420.08	0.5	0.050						
422.55	1.2	0.054						
423.99	0.4	0.141						
424.72	0.6	0.307						
425.62	0.5	0.105						
426.90	0.4	0.041						
428.20	0.5	0.092						
430.48	0.9	0.701						
431.47	0.6	0.267						
434.17	0.3	0.038						
439.94	0.3	0.036						
442.58	0.4	0.018						
444.29	0.9	0.010						
446.04	0.3	0.017						
450.11	0.3	0.019						
451.52	0.5	0.007						
455.19	0.3	0.034						

(B) = Blended peak. Assignments only apply to the peaks that are detected in the spectra of the irradiated sample. + = cation; - = anion.

respectively. VUV photolysis leads to the formation of three new absorption features that appear in the spectrum at 525.6 nm, 562.5 and 574.8 nm respectively. A Ne/NO_2 matrix experiment clearly indicates that the band at 574.8 nm can be assigned to absorption by the anion ($C_{44}H_{20}^-$). Band peak positions, intensities and *FWHM* are reported in Table 7.

4.8. Neutral and ionized dicoronylene $C_{48}H_{20}$

The absorption spectra of neutral and ionized dicoronylene have recently been studied in detail (Chen et al. 2001). The results are briefly reviewed here. The spectrum of neutral dicoronylene (Fig. 9) isolated in a neon matrix exhibits three structured band systems around 248.3, 333.3 and 444.6 nm. These band systems are all depleted upon irradiation of the neutral dicoronylene. Seven new peaks appear in the spectrum upon photolysis. The spectrum of the ion is clearly dominated by two strong bands peaking at 682.5 nm and 1017.1 nm. Comparison with a Ne/NO_2 matrix indicates that all the new peaks can be assigned to the cation, $C_{48}H_{20}^+$. All the results are in agreement with previous observations (Chen et al. 2001). Band peak positions, intensities and *FWHM* are reported in Table 8.

5. Comparison with the diffuse interstellar bands

The position of the bands measured in the laboratory spectra of neutral and ionized PAHs are compared with DIB data in Table 9. The comparison is limited to band peak positions and relative band peak intensities since the interaction with the solid matrix leads to a broadening of intrinsic band profiles that

Table 4. Absorption features associated with the UV/Vis/NIR spectra of neutral and ionized decacyclene ($C_{36}H_{18}$) isolated at 4 K in inert-gas matrices.

Neutral in neon matrix			10 min. irr. in neon matrix			10 min. irr. in neon/NO_2 matrix		
Peak pos. (nm)	*FWHM* (nm)	Abs_{max}	Peak pos. (nm)	*FWHM* (nm)	Abs_{max}	*FWHM* (nm)	Abs_{max}	Assignment
213.51 (B)	25.3	0.414	532.92	35.4	0.010	34.2	0.026	+
251.78 (B)	20.8	0.204	814.67	42.9	0.008	64.5	0.024	+
275.30 (B)	4.1	0.148	1083.32	74.8	0.010	53.9	0.022	+
284.79 (B)	5.5	0.148						
297.14 (B)	7.8	0.110						
310.67 (B)	5.1	0.153						
326.42 (B)	3.6	0.219						
346.54 (B)	7.9	0.224						
364.21 (B)	9.2	0.275						
392.20 (B)	12.7	0.148						
401.51 (B)	1.9	0.114						
406.01 (B)	4.1	0.116						
410.51 (B)	1.5	0.111						
412.00 (B)	0.3	0.110						
414.82 (B)	0.8	0.122						
419.02 (B)	4.2	0.085						
424.15 (B)	4.6	0.055						
428.72 (B)	0.8	0.047						
433.53 (B)	1.0	0.014						
439.01 (B)	1.0	0.007						
443.78 (B)	0.8	0.051						
448.84 (B)	1.0	0.018						
454.52 (B)	0.9	0.010						

(B) = Blended peak. Assignment only apply to the peaks that are detected in the spectra of the irradiated sample. + = cation.

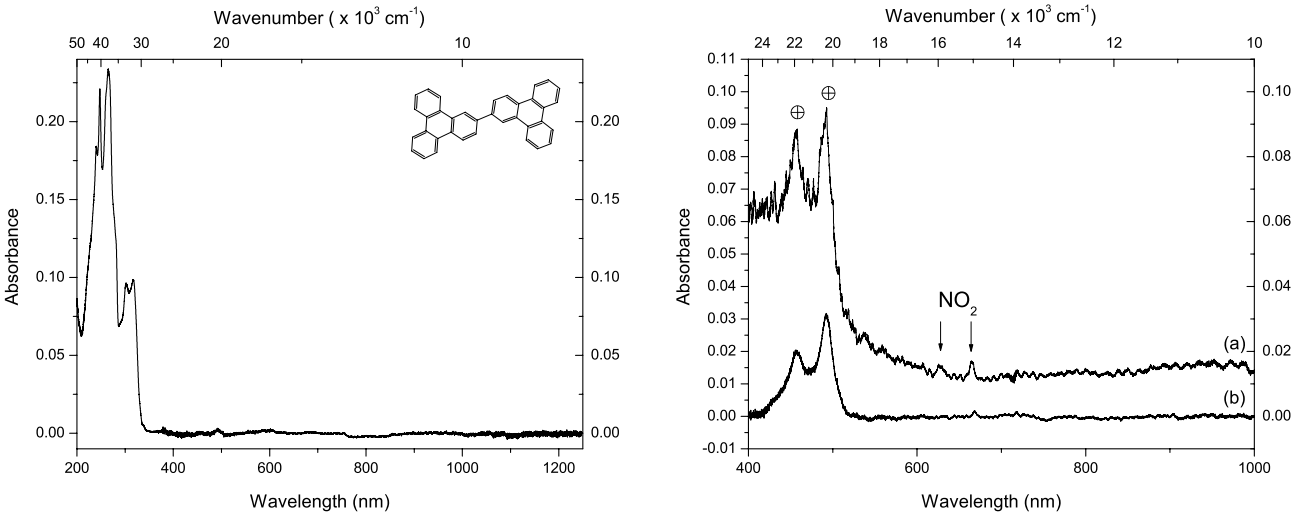

Fig. 6. Comparison of the spectral features associated with neutral (left panel) and VUV-irradiated (right panel) 2, 2′-bis-triphenylyl (Tp) isolated in neon (Ne) and in Ne/NO_2 matrices. **a)** is the spectrum of the photolysis products in a neon/NO_2 matrix; **b)** is the spectrum of the photolysis products in a neon matrix. Band peak positions, intensities and *FWHM* are given in Table 5.

prevents further comparison with astronomical data (Salama 1996; Salama et al. 1999). In Table 9 we have applied the criteria that have been used in our previous studies (Salama et al. 1999) when comparing MIS laboratory spectra with astronomical data. In the case of neutral PAHs we have taken into account all DIBs that fall in a window of ∼0.25% in fractional energy to the blue of the PAH band peak energy as measured in the matrix. In the case of ionized PAHs, we have taken into account all DIBs that fall in a window of ∼0.5% in fractional energy to the blue of the PAH ion band peak energy as measured in the matrix.

These criteria have been chosen to take into account the upper limit of the energy shift that is expected to be induced by the solid matrix environment on isolated PAH molecules and ions

Table 5. Absorption features associated with the UV/Vis/NIR spectra of neutral and ionized 2, 2′-bis-triphenylyl ($C_{36}H_{22}$), isolated at 4 K in inert-gas matrices.

Neutral in neon matrix			10 min. irr. in neon matrix			10 min. irr. in neon/NO_2 matrix		
Peak pos. (nm)	*FWHM* (nm)	Abs_{max}	Peak pos. (nm)	*FWHM* (nm)	Abs_{max}	*FWHM* (nm)	Abs_{max}	Assignment
247.45 (B)	3.5	0.219	457.69	33.3	0.018	31.6	0.034	+
263.97 (B)	21.0	0.228	490.39	16.4	0.027	15.1	0.051	+
303.61 (B)	17.5	0.095						
315.55 (B)	17.6	0.082						

(B) = Blended peak. Assignments only apply to the peaks that are detected in the spectra of the irradiated sample. + = cation.

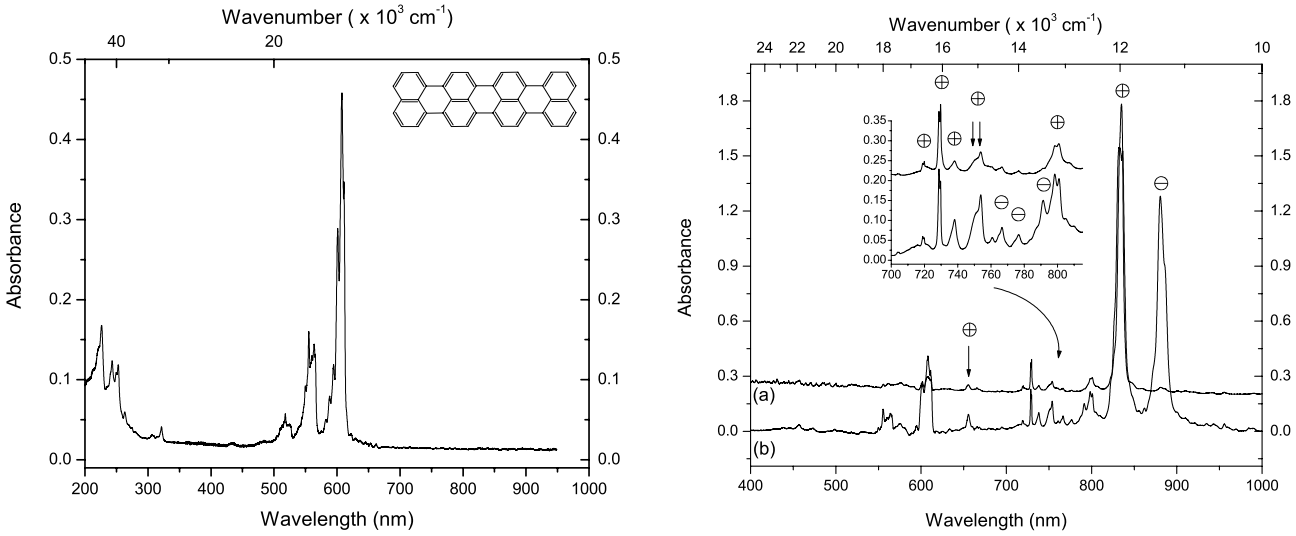

Fig. 7. Comparison of the spectral features associated with neutral (left panel) and VUV-irradiated (right panel) quaterrylene (Qt) isolated in neon (Ne) and in Ne/NO_2 matrices. **a)** is the spectrum of the photolysis products in a neon/NO_2 matrix; **b)** is the spectrum of the photolysis products including, Qt^+ and Qt^-, in a neon matrix. Band peak positions, intensities and *FWHM* are given in Table 6.

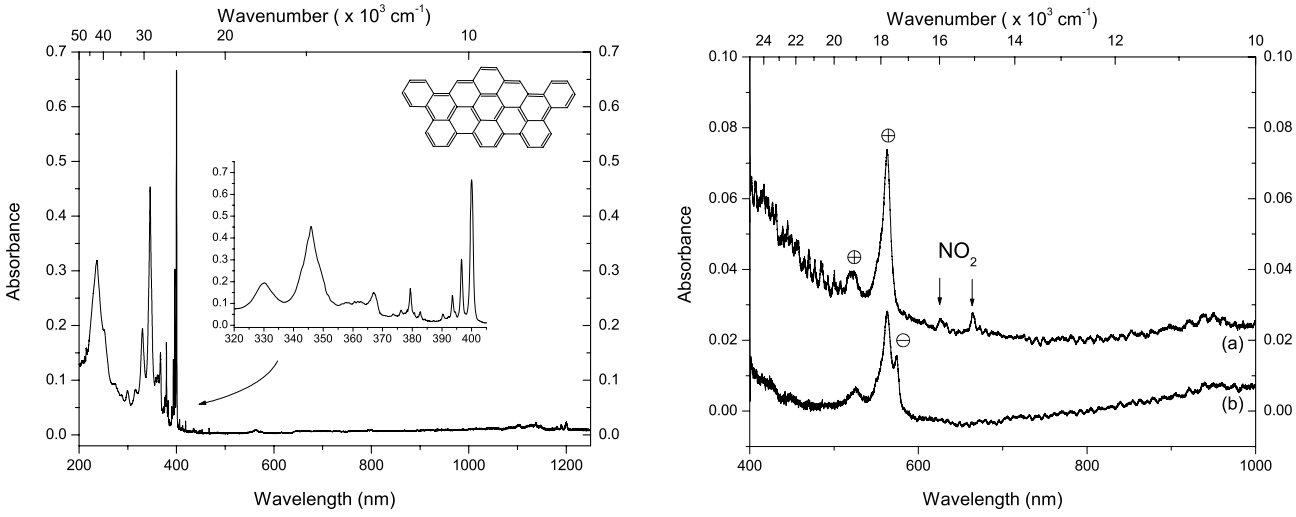

Fig. 8. Comparison of the spectral features associated with neutral (left panel) and VUV-irradiated (right panel) hexabenzo (a, cd, fgh, jk, m, qrs)peropyrene (Hp) isolated in neon (Ne) and in Ne/NO_2 matrices. **a)** is the spectrum of the photolysis products in a neon/NO_2 matrix; **b)** is the spectrum of the photolysis products, including Hp^+ and Hp^-, in a neon matrix. Band peak positions, intensities and *FWHM* are reported in Table 7.

Table 6. Absorption features associated with the UV/Vis/NIR spectra of neutral and ionized quaterrylene ($C_{40}H_{20}$) isolated at 4 K in inert matrices.

Neutral in neon matrix			10 min. irr. in neon matrix			10 min. irr. in neon/NO_2 matrix		
Peak pos. (nm)	*FWHM* (nm)	Abs_{max}	Peak pos. (nm)	*FWHM* (nm)	Abs_{max}	*FWHM* (nm)	Abs_{max}	Assignment
206.41	81.9	0.080	456.44	4.5	0.034	10.9	0.275	+
213.02	3.9	0.010	471.13	10.0	0.014			-
221.75	7.0	0.043	655.56	2.9	0.091	3.3	0.053	+
226.76	3.5	0.059	729.00	1.5	0.220	1.8	0.175	+
244.57	11.4	0.025	737.68	3.2	0.096	3.1	0.047	+
242.81	3.4	0.021	750.88	7.4	0.104	3.8	0.020	+
249.57	2.4	0.022	753.90	0.3	0.098	3.3	0.040	+
252.93	2.7	0.046	760.56	2.9	0.020	4.0	0.018	+
263.50	2.7	0.014	764.65	2.0	0.017	2.8	0.008	+
307.34	5.5	0.006	766.64	2.3	0.044			-
315.59	5.2	0.005	776.39	2.7	0.063			-
321.47	3.6	0.016	791.55	4.1	0.143			-
433.60	13.2	0.006	798.97	5.7	0.209	5.7	0.091	+
516.55	13.5	0.015	833.66	9.0	1.629	5.7	1.577	+
517.96	1.7	0.006	881.84	9.5	1.223			-
525.33	4.4	0.005	939.16	9.7	0.010	9.7	0.010	+
540.59	8.6	0.003	955.94	4.2	0.012	4.2	0.012	+
551.59	8.5	0.052	990.13	4.4	0.007	4.4	0.007	+
555.26	1.8	0.048	1030.56	4.0	0.097	4.1	0.039	+
560.85	7.7	0.084	1073.03	3.5	0.103	3.7	0.054	+
564.98	3.2	0.050						
582.33	7.0	0.031						
588.02	3.4	0.045						
594.67	6.0	0.096						
600.74	3.3	0.226						
607.88	6.2	0.420						
611.65	1.3	0.100						
621.57	6.3	0.016						
629.54	4.6	0.009						
636.59	6.4	0.008						
645.88	6.2	0.006						
653.68	3.2	0.005						
661.77	4.1	0.005						

Assignments only apply to the peaks that are detected in the spectra of the irradiated sample. + = cation; - = anion.

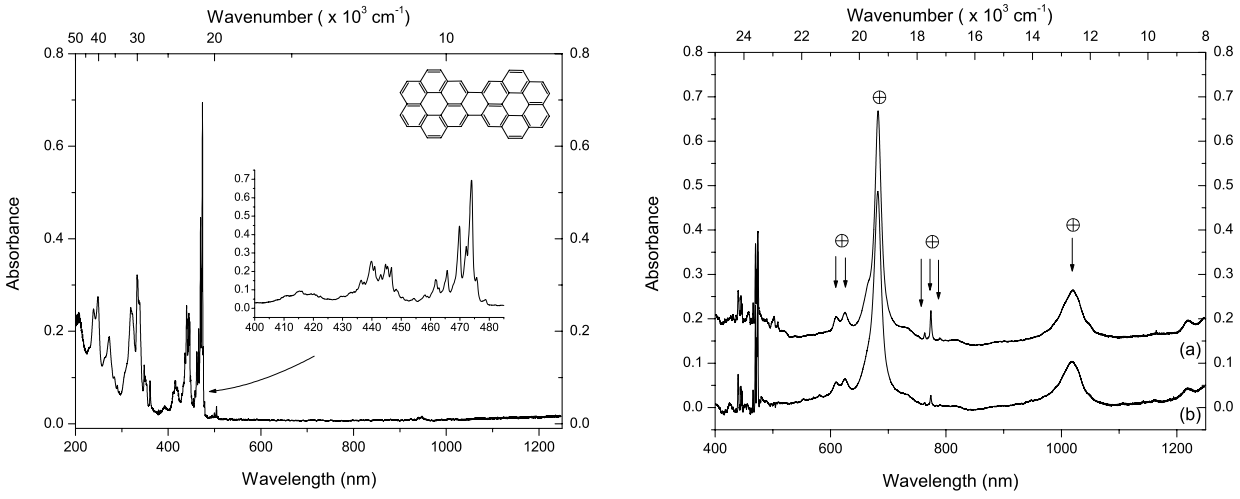

Fig. 9. Comparison of the spectral features associated with neutral (left panel) and VUV-irradiated (right panel) dicoronylene (Dc) isolated in neon (Ne) and in Ne/NO_2 matrices. **a)** is the spectrum of the photolysis products in a neon/NO_2 matrix; **b)** is the spectrum of the photolysis products in a neon matrix. Band peak positions, intensities and *FWHM* are given in Table 8.

Table 7. Absorption features associated with the UV/Vis/NIR spectra of neutral and ionized hexabenzoperopyrene ($C_{44}H_{20}$), at 4 K in inert-gas matrices.

Neutral in neon matrix			10 min. irr. in neon matrix			10 min. irr. in neon/NO_2 matrix		
Peak pos. (nm)	*FWHM* (nm)	Abs_{max}	Peak pos. (nm)	*FWHM* (nm)	Abs_{max}	*FWHM* (nm)	Abs_{max}	Assignment
236.02 (B)	21.3	0.298	525.63	21.3	0.006	19.4	0.01	+
299.38 (B)	4.1	0.081	562.47	17.2	0.028	10.3	0.045	+
315.99 (B)	5.8	0.084	574.83	3.0	0.009			-
330.26 (B)	6.0	0.189						
345.87 (B)	5.3	0.411						
357.97 (B)	2.9	0.104						
361.81 (B)	6.2	0.108						
366.72 (B)	3.9	0.142						
373.67	0.8	0.051						
376.28	0.7	0.068						
379.35	0.7	0.158						
382.65	0.6	0.060						
390.38	0.5	0.052						
393.57	0.6	0.136						
396.63	0.6	0.294						
400.02	1.0	0.675						
406.37	0.7	0.028						
412.65	0.3	0.017						
418.71	0.7	0.021						
435.11	1.5	0.011						
1180.70	2.0	0.014						
1189.90	2.2	0.018						
1199.90	3.5	0.022						

B) = Blended peak. Assignment only apply to the peaks that are detected in the spectra of the irradiated sample. + = cation; - = anion.

(Salama 1996; Romanini et al. 1999). The estimate of the blue shift in peak position induced by the matrix – as opposed to the gas phase – is based on the limited information that is currently available on the spectra of PAH ions in the gas phase (Romanini et al. 1999; Bréchignac & Pino 1999; Biennier et al. 2002). Of all the available DIB data we have deliberately chosen to only use data from one astronomical object, HD183143. The reason for this choice is that this object, being the source of extensive studies by many independent observers, is the best studied DIB object and can thus be used for reliable comparisons with the laboratory data. Finally, note that the coincidences that are found between PAH bands and specific DIBs do not imply that detection can be secured. They provide, however, a powerful and unique tool to select potential DIB carrier molecules that can be subsequently tested in an unambiguous way through gas phase studies in a free jet environment that provide information on intrinsic band profiles.

5.1. Comparison of diphenanthrofuran bands with the observed DIBs

Neutral diphenanthrofuran absorption bands do not correspond to any known DIB. A comparison of the DIB positions with the spectra of the diphenanthrofuran ions indicates that the position of the strongest cation band that peaks at 4444 Å in matrix (predicted near 4422 Å in the gas phase) comes close to the DIB λ 4427.96. Six weaker DIBs: λ 6302.29, λ 6308.92, λ 6311.53, λ 6317.75, λ 6324.81 and λ 6330.14, come also close to the second strongest absorption of the diphenanthrofuran cation that peaks at 6332 Å (predicted near 6300 Å in the gas phase). Of these 6 DIBs only the first two are within 10 Å of the calculated gas-phase peak positions.

The relative intensities of the two stronger cation absorption bands are 4444 : 6332 Å = 1 : 0.96. None of the six DIBs that fall close to the 6332 Å absorption band of the diphenanthrofuran cation presents the required intensity to match the band ratio measured in the laboratory. For example, the relative intensities of the two DIBs that most closely match the expected gas-phase positions are 4427.96 : 6302.29 Å = 1 : 0.04. Thus, despite the close agreement found in wavelength positions between the two stronger bands of the diphenanthrofuran cation and two DIBs, it is clear that the relative intensities differ considerably, ruling out this PAH ion as potential DIB carrier. (Note that the relative band intensities associated with specific PAH species are similar in solid matrices and in the gas phase (Romanini et al. 1999; Bréchignac & Pino 1999)).

Finally, we note that the weak absorption that is associated with the diphenanthrofuran anion and that is measured at 7528 Å (predicted at 7491 Å in the gas phase) comes close to the weak 7493 Å DIB.

5.2. Comparison of terrylene bands with the observed DIBs

Neutral terrylene absorption bands do not correspond to any known DIB. The two stronger features of the terrylene cation

Table 8. Absorption features associated with the UV/Vis/NIR spectra of neutral and ionized dicoronylene ($C_{48}H_{20}$), isolated at 4 K in inert-gas matrices.

Neutral in neon matrix			10 min. irr. in neon matrix			10 min. irr. in neon/NO_2 matrix		
Peak pos. (nm)	*FWHM* (nm)	Abs_{max}	Peak pos. (nm)	*FWHM* (nm)	Abs_{max}	*FWHM* (nm)	Abs_{max}	Assignment
238.80 (B)	5.9	0.249	610.01	9.3	0.055	7.8	0.050	+
248.30 (B)	6.4	0.276	625.18	12.6	0.063	14.9	0.060	+
272.81 (B)	8.2	0.187	664.30	15.0	0.126	13.3	0.124	+
283.26 (B)	6.3	0.102	682.46	12.8	0.456	12.1	0.485	+
290.21 (B)	2.4	0.082	762.63	3.9	0.010	2.5	0.014	+
293.77 (B)	1.8	0.069	773.71	2.7	0.025	2.6	0.064	+
306.67 (B)	6.9	0.103	1017.1	26.3	0.103	34.0	0.109	+
319.20 (B)	11.9	0.251						
333.33 (B)	4.3	0.317						
338.64 (B)	4.4	0.247						
348.14 (B)	1.2	0.127						
350.99 (B)	8.0	0.103						
360.88 (B)	1.2	0.092						
392.80	8.6	0.036						
436.23	0.8	0.150						
437.43	0.9	0.139						
439.74	1.2	0.254						
440.98	0.6	0.226						
442.95	0.6	0.182						
444.60	0.7	0.240						
445.39	0.5	0.225						
446.55	0.8	0.220						
450.39	1.0	0.060						
454.30	1.0	0.053						
458.03	0.7	0.072						
458.99	0.4	0.064						
461.78	0.7	0.158						
462.95	0.7	0.112						
465.74	0.6	0.204						
469.74	0.8	0.438						
472.15	1.0	0.333						
473.85	0.9	0.698						
495.02	1.6	0.018						
499.62	1.1	0.023						
504.18	1.3	0.035						

(B) = Blended peak. Assignments only apply to the peaks that are detected in the spectra of the irradiated sample. + = cation.

fall at 6904 and 7039 Å with a relative intensity of 1 : 0.2. The predicted positions for these 2 bands in the gas phase are 6870 and 7004 Å respectively. The closest counterparts in the DIB spectrum fall at 6886.92 and 7004.30 Å, respectively, with a relative intensity of 1 : 0.07. This close correlation -within the uncertainties attached to the astronomical measurements of weak DIBs- makes the terrylene cation a promising candidate for further gas-phase studies.

Finally, the strongest (0.722 *Abs*) anion feature measured at 7413 Å in the laboratory (predicted near 7376 Å in the gas phase) coincides with the λ 7375.90 DIB. The two other, weaker, spectral features associated with the anion and measured in the laboratory at 9015 and 10012 Å, respectively, are of similar intensity (0.086 and 0.088 *Abs*, respectively) with a relative intensity of 1 : 0.12 with the strongest, 7413 Å, anion band. Any DIBs correlated with these 2 bands would thus be expected to be found at the 0.002 *Abs* level that is barely at the detection limit. Moreover, the 2 bands fall in a wavelength region that is astronomically not well explored. We thus conclude that the case is still open and that, if further verified, only the λ 7375.90 DIB might be correlated with the terrylene anion, the wavelength agreement that is observed between the 10012 Å laboratory band with the λ 9955.90 DIB being purely coincidental.

5.3. Comparison of ovalene bands with the observed DIBs

In this case, the measurements were compared with the spectrum previously published by Ehrenfreund et al. (1992). Some discrepancy was found in the case of the neutral molecule. Comparison of the spectral data between the two studies

Table 9. Comparison of confirmed DIBs towards HD183143 with band peak positions of neutral (0) PAHs and PAH cations (+) and anions (–).

λ PAH (Å)	Abs_{max}	λ PAH (gas) (Å)	λ HD183143 (Å)	Abs_{max}	Ref.
4444 DiFurA+	0.055	4422	4427.96	0.141	BB37
6332 DiFurB+	0.053	6300	6302.29	0.006	OT00
			6308.92	0.038	HL91
			6311.53	0.017	He75
			6317.75	0.020	JD93
			6324.81	0.018	JD93
			6330.14	0.018	JD93
7528 DiFurA-	0.006	7491	7492.93	0.004	VF02
4848 TerC0	0.328	4836			
5135 TerD0	0.314	5122			
5198 TerB0	0.637	5185			
5263 TerA0	0.951	5250			
6646 TerE+	0.123	6613	6613.63	0.075	Me34
			6622.59	0.006	K95
			6632.86	0.007	JD94
			6635.50	0.003	K95
			6644.33	0.009	OT00
6707 TerC+	0.293	6674	6684.83	0.002	OT00
			6686.46	0.002	OT00
			6689.38	0.008	K95
			6694.40	0.004	JD94
			6699.28	0.023	Sa78
			6701.87	0.009	Fe83
			6707.73	0.002	OT00
6904 TerA+	1.908	6870	6886.92	0.073	HL91
7039 TerB+	0.358	7004	7004.30	0.005	VF02
7413 TerA-	0.722	7376	7375.90	0.017	JD94
			7385.92	0.026	JD94
			7391.48	0.003	VF02
			7401.71	0.015	JD94
			7405.77	0.014	JD94
			7406.35	0.017	JD94
8704 TerD+	0.162	8661			
9015 TerC-	0.086	8970			
9667 TerF+	0.091	9619			
10012 TerB-	0.088	9962	9955.90	0.043	VF02
			9971.07	0.028	VF02
4256 OvaC0	0.105	4246			
4305 OvaA0	0.701	4294			
4543 OvaF+	0.010	4520			
4632 OvaA+	0.097	4609			
719 OvaE+	0.010	4696			
5260 OvaD+	0.011	5234	5236.34	0.030	OT00
			5247.91	0.015	OT00
5357 OvaA-	0.015	5330	5349.16	0.007	OT00
5621 OvaC+	0.014	5593	5594.54	0.012	OT00
			5597.38	0.002	OT00
			5600.49	0.008	OT00
			5609.96	0.011	JD94
8082 OvaI+	0.003	8042			
8574 OvaH+	0.006	8531	8530.79	0.04	JD94
8696 OvaG+	0.008	8652			
9749 OvaB+	0.031	9701			

Table 9. continued.

λ PAH (Å)	Abs_{max}	λ PAH (gas) (Å)	λ HD183143 (Å)	Abs_{max}	Ref.
5329 DecaA+	0.010	5303			
8147 DecaB+	0.008	8106	8104.89	0.017	VF02
10833 DecaC+	0.010	10779			
4577 TPhenB+	0.012	4554			
4904 TPhenA+	0.019	4880	4882.56	0.064	Wi58
5609 QuaTC0	0.084	5595	5594.54	0.012	OT00
			5597.38	0.002	OT00
			5600.49	0.020	OT00
			5609.96	0.010	JD94
5947 QuaTB0	0.096	5932	5945.53	0.012	K95
			5947.29	0.017	K95
6079 QuaTA0	0.420	6063	6065.19	0.017	JD94
			6068.45	0.005	OT00
			6071.08	0.007	JD94
7290 QuaTB+	0.220	7254	7274.50	0.017	JD94
7509 QuaTD+	0.072	7471			
7916 QuaTB-	0.143	7876	7904.92	0.015	VF02
			7915.13	0.022	JD94
7990 QuaTC+	0.209	7950	7951.25	0.010	VF02
			7987.89	0.026	JD94
8337 QuaTA+	1.629	8295			
8818 QuaTA-	1.223	8775			
5256 HBenzE+	0.006	5230	5236.34	0.026	OT00
			5247.91	0.015	OT00
			5349.16	0.007	OT00
5625 HBenzA+	0.028	5597	5597.38	0.002	OT00
			5600.49	0.008	OT00
			5609.96	0.011	JD94
5748 HBenzB-	0.015	5720	5719.68	0.020	JD94
			5746.21	0.017	JD94
4398 DicoC0	0.254	4386			
4446 DicoD0	0.240	4435			
4630 DicoE0	0.112	4618			
4657 DicoB0	0.438	4646			
4739 DicoA0	0.698	4727	4726.35	0.063	He75
			4728.35	0.027	He75
6100 DicoD+	0.055	6070	6071.08	0.007	JD94
			6084.94	0.009	OT00
			6089.79	0.035	HL91
6252 DicoC+	0.063	6221	6220.86	0.008	K95
			6223.53	0.017	JD94
			6226.02	0.007	K95
			6234.01	0.023	He75
			6236.71	0.008	JD93
			6244.42	0.024	OT00
			6245.36	0.010	K95
			6250.77	0.006	OT00
6825 DicoA+	0.456	6791	6792.54	0.029	He88
			6795.18	0.016	He88
			6801.39	0.016	He88
			6804.82	0.004	He88
			6811.30	0.019	He88
			6812.39	0.019	He88
7737 DicoE+	0.025	7699	7702.32	0.003	VF02
			7705.90	0.024	JD94
			7709.67	0.017	JD94
			7713.49	0.014	JD94
			7721.03	0.048	HL91

Table 9. continued.

λ PAH (Å)	Abs_{max}	λ PAH (gas) (Å)	λ HD183143 (Å)	Abs_{max}	Ref.
			7727.95	0.005	VF02
			7730.19	0.004	VF02
10171 DicoB+	0.103	10120	10130.33	0.066	VF02
			10139.24	0.063	VF02
			10145.67	0.030	VF02
			10148.70	0.029	VF02
			10152.62	0.027	VF02
			10158.61	0.047	VF02
			10164.55	0.042	VF02

λ PAH (gas) corresponds to the laboratory wavelength that has been blue shifted by 0.25% and 0.5% in energy to account for the blue shift in energy that is expected for cold gas phase neutral and ionic PAHs, respectively, and is derived from the case studies of naphthalene (Salama & Allamandola 1991; Romanini et al. 1999) and phenanthrene (Bréchignac & Pino 1999). DiFur: diphenanthrofuran, $C_{28}H_{16}O$; Ter: terrylene, $C_{30}H_{16}$; Ova: ovalene, $C_{32}H_{14}$; Deca: decacyclene, $C_{36}H_{18}$; TPhen: 2, 2′-bis- triphenylyl, $C_{36}H_{22}$; Quat: quaterrylene, $C_{40}H_{20}$; HBenz: hexabenzoperopyrene, $C_{44}H_{20}$; Dico: dicoronylene, $C_{48}H_{20}$. A = Strongest absorption band in the VUV-NIR range, B = second strongest absorption band, and so forth; + = cation, - = anion, 0 = neutral band. All listed DIB features are observed towards source HD183143 and taken from O'Tuairisg et al. 2000 for DIBs with 4000 nm $< \lambda \leq$ 6812 nm, Jenniskens et al. (1994) for DIBs with 4000 nm $< \lambda <$ 8648 nm, and from Vuong & Foing (2002) for DIBs with $\lambda >$ 7000 nm. References indicate the original description of the features. Abs_{max} for DIBs is defined as the line center depth and is related to the equivalent width as $EW \sim FWHM\times$ center depth. The limit of detection of the center depth is 2.5×10^{-3} for a 2 Å wide DIB with EW detection limit 5 mA. Detailed discussion on errors in EW values for DIBs can be found in O'Tuairisg et al. (2000) and in Cami et al. (1997). Reference codes: BB37- Beals & Blanchet (1937), Fe83- Ferlet et al. (1983), GA00- Galazutdinov (2000), He67- Herbig (1967), He75- Herbig (1975), He88- Herbig (1988), HL91- Herbig & Leka (1991), JD93- Jenniskens & Deśert (1993), JD94- Jenniskens & Deśert (1994), K95- Krelowski et al. (1995), Me34- Merril (1934), Sa78- Sanner et al. (1987), OT00- O'Tuairisg et al. (2000), VF02- Vuong & Foing (2002), Wi58- Wilson (1958).

indicates that the data for neutral ovalene that are presented in this work exhibit additional, narrower, peaks. Since these peaks were unresolved in the Ehrenfreund et al. study we conclude that the spectrum that is presented here for the neutral molecule is more representative, and we thus base our conclusions on these most recent results. Total agreement is found between the two studies when comparing the spectra of the ion.

None of the neutral bands match any known DIBs. Similarly, the two strongest ovalene cation features have no DIB counterparts. Although the third and fourth strongest cation peaks come close to known DIBs, the associated relative intensities do not match the laboratory measurements lead to 5621 : 5260 Å = 1 : 0.8 compared to 5594.54 : 5236.34 Å = 1 : 2.5 for the corresponding DIBs. These findings thus rule out the ovalene cation as a potential DIB carrier.

We note that the only absorption band that is associated to the anion in the laboratory spectra and measured at 5357 Å (predicted at 5330 Å in the gas phase) falls close to the weak (0.007 *Abs*) λ 5349 DIB. The strong cation band at 9749 Å that is observed in the lab spectra is shifted 30 Å compared to the measurement by Ehrenfreund et al. (1992) (which is probably due to saturation making an exact determination of the wavelength position impossible). However, there is no counterpart for this band in the DIB spectra (Ehrenfreund et al. 1995).

5.4. Comparison of decacyclene bands with the observed DIBs

None of the bands of neutral decacyclene match any known DIBs. The cation spectrum shows three broad absorption features of equal intensities (about 0.01 *Abs*). The band measured at 8147 Å (predicted at 8106 Å in the gas phase) coincides with the λ 8104.89 DIB. The poor quality of the laboratory spectrum in this case prohibits further conclusions and the case is pending future gas-phase experiments.

5.5. Comparison of 2, 2′-bis-triphenylyl bands with the observed DIBs

Neutral triphenylyl absorb in the UV where no DIBs have been detected. The two visible absorption features associated with the triphenylyl cation have relative intensities 4904 : 4577 Å = 1 : 0.6 and fall in the DIB region. The strongest of the two bands falls at 4904 Å (4880 Å predicted gas-phase value) and is close to the λ 4882.56 DIB. No DIB counterpart is found, however, for the second strongest band that falls at 4577 Å (4554 Å in the gas-phase). If the λ 4882.56 DIB (0.064 *Abs* in HD183143) were indeed associated with the triphenyl cation, a second, weaker, DIB (0.038 *Abs* in HD183143) should be detected near 4550 Å. The absence of any DIB at this wavelength seems to rule out the triphenylyl cation as a potential DIB carrier.

5.6. Comparison of quaterrylene bands with the observed DIBs

Neutral quaterrylene absorbs in the DIB range. The strongest features of neutral quaterrylene measured in the MIS spectra fall at 6079, 5947 and 5609 Å with relative intensities = 1 : 0.23 : 0.20. The DIBs that most closely match the intensity ratio of these neutral features at the predicted gas phase wavelengths

are λ 6065.19, λ 5945.53 and λ 5597.38 with relative intensities = 1 : 0.7 : 0.12. This is marginally in agreement considering the uncertainties associated with DIB strength measurements.

No DIBs are found near the positions of the strongest cation and anion absorption features that fall at 8337 Å and 8818 Å respectively in Ne matrices (8295 Å and 8775 Å respectively in the gas phase) making the quaterrylene cation and anion unlikely DIB carriers.

5.7. Comparison of hexabenzoperopyrene bands with the observed DIBs

None of the features associated with the neutral spectrum of hexabenzoperopyrene falls in the DIB region (∼4000−10 000 Å). The three absorption bands associated with the ions (2 for the cation and 1 for the anion) fall, however, in the DIB range and can potentially be matched with eight DIBs when taking into account the projected peak positions in the gas phase. The two cation peaks are measured at 5625 Å and 5256 Å in Ne matrices with a relative intensity ratio = 1 : 0.2. Three DIBs are found in the wavelength window associated with the strongest cation band at 5625 Å (5597 Å projected value in the gas-phase). They are the λ 5597.38, λ 5600.49 and λ 5609.96 DIBs with intensities of 0.002, 0.008 and 0.011 *Abs*, respectively. Thus, in the best scenario case, where the strongest of the 3 DIBs (the λ 5609.96 DIBs of 0.011 *Abs*) is correlated to the hexabenzoperopyrene cation, a DIB at the 0.002 *Abs* level is expected near the position of the second strongest band of the cation, a level that is barely at the detection limit.

We thus conclude that the case is still open. Only one of the λ 5597.38, λ 5600.49 and λ 5609.96 DIBs might be correlated with the hexabenzoperopyrene cation. The wavelength agreement that is observed between the 5256 Å cation band and the λ 5236.3, λ 5247.9 and λ 5349.1 DIBs is purely coincidental. Thus, any correlation between the hexabenzoperopyrene cation and the DIBs must, if confirmed, be limited to the strongest cation band (5625 Å in MIS and 5597 Å expected in the gas phase).

Finally, the only band associated with the hexabenzoperopyrene anion in the laboratory spectra falls at 5748 Å (5720 Å in the gas phase) and can potentially be matched by either the λ 5719.68 or the λ 5746.21 DIB.

5.8. Comparison of dicoronylene bands with the observed DIBs

The strongest absorption band of neutral dicoronylene measured at 4739 Å in matrix (4727 Å projected value in the gas phase) comes close to two DIBs falling at 4726.35 and 4728.35 Å respectively. No DIBs are found near the other strong absorption band of neutral dicoronylene making the neutral molecule an unlikely DIB carrier.

The strongest cation absorption band measured at 6825 Å in matrix (6791 Å in the gas phase) dominates clearly the spectrum with an intensity of 0.456 *Abs*. Among all the 6 DIBs that potentially match this band in terms of peak position, the λ 6792.54 DIB (0.029 *Abs*) provides the closest correspondence. The band intensity ratio with the next strongest band of the dicoronylene cation (10 171 Å in MIS) is 1:0.23. Thus any DIB correlated with the second strongest cation band is predicted to have intensity ranging from 0.007 (detectable if not obscured by other band) to 0.001 (below detection limit) *Abs*. It is clear that none of the 7 DIBs associated with the 10 171 Å band of the dicoronylene cation in Table 9 meets this requirement.

The wavelength agreement that is observed between 10 171 Å cation band and the DIBs detected around 1 μm is purely coincidental. We also note that the spectral region around 1 μm is not well explored in astronomical observations.

Thus, any assignment between the dicoronylene cation and the DIBs must, if confirmed, be limited to the strongest cation band (6825 Å in MIS and 6791 Å in the gas phase).

6. Conclusion

Astronomical data obtained with the ISO satellite have provided evidence for the presence of PAHs of molecular sizes larger than was previously assumed (∼50 C atoms) as well as 5-ring PAH structures (Tielens et al. 1999). We have therefore measured large (C_{28}–C_{48}) PAHs, with condensed and open structures, including pentagons and heteroatoms, and measured the absorption spectra, in the UV-NIR range, of the neutral and ionized forms when isolated in cold (5 K), inert-gas, matrices.

The promising candidates for future gas-phase experiments are those neutral and ionized PAHs that possess one or more bands that match DIB features in the wavelength comparison window. In summary, the MIS laboratory data obtained in this work indicate that some large neutral and ionized PAH are promising candidates for the DIB carriers. Out of a laboratory set of 21 PAH species (including 8 neutral PAHs, 8 PAH cations and 5 PAH anions) which sample compact and non-compact PAHs, and PAHs with a heteroatom, 8 exhibit a possible coincidence with DIBs, 1 cannot be settled, and 12 can be excluded as potential DIB carriers. The gas-phase, jet, experiments which are now being developed (Biennier et al. 2002) will provide the much needed data to definitively assess the validity of the PAH proposal with regards to the DIBs. More astronomical surveys of DIB objects are also needed, especially in the wavelength ranges that have not been as yet frequently observed.

A few general remarks can be derived from this laboratory study of large PAHs. First, terrylene, ovalene, hexabenzoperopyrene, quaterrylene and dicoronylene each exhibits a strong cation absorption feature that clearly dominates the spectrum in the 400–1000 nm range. The observation of this spectral characteristic of PAH ions confirms the predictions that had been previously made for the PAH-DIB model based on the study of smaller-size PAHs (Salama et al. 1996). Similarly, a displacement toward the red is observed for the absorption of PAHs included within the same chemical subclass (e.g., perylene (Joblin et al. 1999), terrylene and quaterrylene). All these observations are useful to derive general properties of PAHs in the astrophysical context. For example, one can predict that larger PAHs in the linear series perylene, terrylene and quaterrylene will be difficult to identify with known DIB features since their spectral signature falls into the NIR region, which is difficult to explore from the astronomical point of view. Further

astronomical surveys will be needed to improve the astronomical data in this range.

This comparative study has shown that most neutrals – with the possible exception of quaterrylene – can be definitely excluded as DIB carriers. It has also indicated that the less compact structures, such as diphenanthrofuran, decacyclene and $2,2'$-bis-triphenylyl, can also be excluded from future DIB searches. Several ionized PAHs (cations as well as anions) do however show possible correlations with DIBs. This is the case, for example, of the ions of terrylene, ovalene, hexabenzoperopyrene and dicoronylene. All are compact structures that are expected to be photostable in an extraterrestrial environment (Salama et al. 1996). The coincidences found in this work between the strong absorption bands of neutral quaterrylene, the terrylene ion, the hexabenzoperopyrene ion, and the dicoronylene ion and some DIBs make these specific species interesting candidates for future gas-phase studies.

In conclusion, given the large number of DIBs the probability of close matches between the laboratory and DIB spectra could be due to random chance. In particular since each new high resolution study of DIBs reveals a number of new weak features. We reiterate that a direct comparison of the MIS spectra of these large neutral and ionized PAHs with the spectra of a selected reddened star, HD183143, cannot yield to a decisive, unambiguous, identification of DIB carriers until gas-phase laboratory data are available. This is due to shifts in band peak positions and to band profile broadening induced by the solid matrix in the spectrum of the isolated PAHs. Only gas phase measurements can provide access to intrinsic band positions and profiles that are necessary for the definitive identification of any specific molecular DIB carrier. A comparison between the MIS laboratory data and the astronomical observations is very useful, however, when matrix-to-gas-phase shifts are taken into account. The MIS data provide, then, an essential and unique guide for the selection of PAH ions to be studied under conditions that mimic closely the conditions reigning in the interstellar medium (i.e., in a free jet expansion).

The gas-phase, jet experiments which are just now developed (Biennier et al. 2002) will provide the much-needed data to definitively assess the validity of the PAH proposal with regards to the DIBs. More astronomical surveys of DIB objects are also needed, especially in the wavelength ranges that have not been well observed.

These laboratory experiments have been conducted in support of the experiment "ORGANIC" on the ISS (Ruiterkamp et al. 2001). This experiment will test the photostability of large carbon-bearing molecules during a long duration exposure in Earth orbit. Comparison of these laboratory spectra with the spectra of the post-flight samples will provide important information on the effects of space radiation on cosmic organic materials and will be reported separately.

Acknowledgements. These studies are part of the preparation for the ORGANICS experiment on the European EXPOSE facility on board the International Space Station (ISS). The authors acknowledge useful discussions with Lou Allamandola. RR acknowledges funding from SRON grant MG049. Additional support has been provided by NASA (OSS Space Astrophysics Research and Analysis program) and ESA Space Science Dept.

References

Allamandola, L. J., Tielens, G. G. M., & Barker, J. R. 1989, ApJS, 71, 733
Bakes, E. L. O., & Tielens, A. G. G. M. 1994, ApJ, 427, 822
Beals, G. H., & Blanchet, G. H. 1937, PASP, 49, 224
Bettens, R. P. A., & Herbst, E. 1996, ApJ, 468, 686
Biennier, L., Salama, F., Allamandola, L., Scherer, J., & O'Keefe, A. 2002, to be submitted
Beals, G. H., & Blanchet, G. H. 1937, PASP, 49, 224
Bréchignac, P., & Pino, T. 1999, A&A, 343, L49
Cami, J., Sonnentrucker, P., Ehrenfreund, P., & Foing, B. H. 1997, A&A, 326, 822
Clar, E. 1964, Polycyclic Hydrocarbons (Academic Press, London)
Chen, B., & Salama, F. 2001, J. Chem. Phys., submitted
Chlewicki, G., Groot, M. S., Van der Zwet, G. P., et al. 1987, A&A, 173, 131
Douglas, A. E., & Herzberg, G. 1941, ApJ, 94, 381
Ehrenfreund, P., D'Hendencourt, L., Verstraete, L., et al. 1992, A&A, 259, 257
Ehrenfreund, P., Foing, D'Hendecourt, L., Jenniskens, P., & Desert, F. X. 1995, A&A, 299, 213
Ehrenfreund, P., & Foing, B. H. 1996, A&A, 307, L25
Ehrenfreund, P., & Charnley, S. B. 2000, ARA&A, 38, 427483
Ehrenfreund, P., Sonnentrucker, P., O'Tuairisg, S., Cami, J., & Foing, B. H. 2001, in Proceedings of the Workshop: The Bridge between the Big Bang and Biology, Stromboli 1999, Consiglio Nazionale delle Ricerche of Italy, ed. F. Giovannelli, Special Volume, 150
Ferlet, R., Roueff, E., Horani, M., & Rostas, J. 1983, A&A, 125, L5
Foing, B. H., & Ehrenfreund, P. 1994, Nature, 369, 296
Foing, B. H., & Ehrenfreund, P. 1997, A&A, 317, L95
Freivogel, P., Fulara, J., & Maier, J. P. 1994, ApJ, 431, L151
Galazutdinov, G. A., Musaev, F. A., Krelowski, J., & Walker, G. A. H. 2000, Pubs. of the Astron. Soc. of the Pacific, 112, 648
Henning, Th., & Salama, F. 1998, Science, 282, 2204
Herbig, G. H. 1967, in Radio Astronomy and the Galactic System, IAU Symp., 31, ed. H. van Woerden, 85
Herbig, G. H. 1975, ApJ, 196, 129
Herbig, G. H. 1988, ApJ, 331, 999
Herbig, G. H., & Leka, K. D. 1991, ApJ, 382, 193
Herbig, G. H. 1993, ApJ, 407, 142
Herbig, G. H. 1995, ARA&A, 33, 19
Herbst, E. 1995, Large Molecules in the Interstellar Medium, ASSL Vol. 202, The Diffuse Interstellar Bands, 307
Hudgins, D. M., & Allamandola, L. J. 1999a, ApJ, 516, L41
Hudgins, D. M., & Allamandola, L. J. 1999b, ApJ, 513, L69
Jacox, M. E. 1978, in Rev. Chem. Inter., ed. O. P. Strausz (Verlag Chemie International, Inc.: New York), 1
Jenniskens, P., & Désert, X. 1993, A&A, 274, 465
Jenniskens, P., & Désert, X. 1994, A&A, 106, 39
Joblin, C., Salama, F., & Allamandola, L. 1999, J. Chem. Phys., 110, 7287
Krelowski, J., Sneden, C., & Hiltgen, D. 1995, Plan. Space Sci., 43, 1195
Krelowski, J., Galazutdinov, G. A., & Musaev, F. A. 1998, ApJ, 506, 926
Le Coupanec, P., Rouan, D., Moutou, C., & Léger, A. 1999, A&A, 347, 669
Lucas, R., & Liszt, H. S. 1997, Molecules in Astrophysics: Probes and Processes, ed. E. F. van Dishoeck (Dordrecht: Kluwer), 421
McKelar, A. 1940, Publ. Astr. Soc. Pacific, 52, 187

Mennella, V., Colangeli, L., Brucato, J. R., et al. 1999, Adv. Space Res., 24, 439
Merril, P. W. 1934, PASP, 46, 206
Puget, J. L., & Leger, A. 1989, ARA&A, 27, 161
Romanini, D., Biennier, L., Salama, F., et al. 1999, Chem. Phys. Lett., 303, 165
Ruffle, D. P., Bettens, R. P. A., Terzieva, R., & Herbst, E. 1999, ApJ, 523, 678
Ruiterkamp, R., Ehrenfreund, P., Foing, B., & Salama, F. 2001, Conf. Proc. First European Workshop Exo-/Astro-Biology SP-496, ed. P. Ehrenfreund, O. Angerer, & B. Battrick (ESA), 137
Salama, F., & Allamandola, L. J. 1991 J. Chem. Phys., 94, 6964
Salama, F. 1996, Low Temperature Molecular Spectroscopy, 483, ed. R. Fausto (Kluwer), 169
Salama, F., Bakes, E. L. O., Allamandola, L. J., & Tielens, A. G. G. M. 1996, ApJ, 458, 621
Salama, F. 1999, Solid Interstellar Matter: The ISO Revolution 458, ed. L. d'Hendecourt, C. Joblin, & A. Jones (EDP Sciences, Springer-Verlag, Les Ulis), 65
Salama, F., Galazutdinov, G. A., Krełowski, J., Allamandola, L. J., & Musaev, F. A. 1999, ApJ, 526, 265
Sanner, F., Snell, R., & Vanden Bout, P. 1978, ApJ, 226, 460
Sarre, P. J., Miles, J. R., & Scarrott, S. M. 1995, Science, 269, 674
Sonnentrucker, P., Cami, J., Ehrenfreund, P., & Foing, B. H. 1997, A&A, 327, 1215
Swings, P., & Rosenfeld, L. 1937, ApJ, 86, 483
Tielens, A. G. G. M., & Snow, T. P. (eds.) 1995, The Diffuse Interstellar Bands, IAU Coll. 137 (Kluwer, Dordrecht)
Tielens, A. G. G. M., Hony, S., van Kerckhoven, C., & Peeters, E. 1999, ESA SP-427, The Universe as Seen by ISO, 427, 579
Torres-Godgen, A. V. 1990, PASP, 102, 1406
Ó Tuairisg, S., Cami, J., Foing, B. H., Sonnentrucker, P., & Ehrenfreund, P. 2000, A&A, 142, 225
Tulej, M., Kirkwood, D. A., Pachkov, M., & Maier, J. P. 1998, ApJ, 506, L69
Vuong, M. H., & Foing, B. H. 2000, A&A, 363, L5–L8
Vuong, M. H., & Foing, B. H. 2002, in preparation
Walker, G. A. H., Webster, A. S., Bohlender, D. A., & Krełowski, J. 2001, ApJ, 561, 272
Wilson, R. 1958, ApJ, 128, 57